Modified GaSe Crystals for Laser Systems Applications[1]

Feng-Guang Wu*, Yu.M. Andreev, G.V. Lanskii, V.V. Atuchin**,
T.A. Gavrilova**, and S.Yu. Sarkisov***

Department of Ecological Devises Making, Institute of Monitoring of Climatic and Ecological Systems SB RAS, 10/3, Akademichesky ave., Tomsk, 634055, Russia
Tel.: +7(960) 971-15-40, E-mail: yuandreev@imces.ru
**Key Laboratory of Coherent Light and Atomic and Molecular Spectroscopy of Ministry of Education and College of Physics, Jilin University, 2519 Jie-Fang Road, Changchun, 130023, China*
***Laboratory of Optical Materials and Structures, Institute of Semiconductor Physics SB RAS, 13, Lavrent'ev ave., Novosibirsk, 630090, Russia*
****Semiconductor Materials Science Laboratory, Siberian Physical and Technical Institute of Tomsk State University, 28, Lytkina str., Tomsk, 634050, Russia*

Abstract – Optical properties of *p*-type GaSe and modified solid solution $GaSe_{1-x}S_x$, $x = 0.04–0.412$, crystals were studied to reveal the potentials for phase matching and frequency conversion. First comparative experiment on Er^{3+}:YSGG and CO_2 laser SHG is carried out at room temperature and identical experimental conditions. The temperature phase matching properties for Er^{3+}:YSGG and CO_2 laser SHG in GaSe and mixed $GaSe_{1-x}S_x$, $x = 0.09$, 0.175, and 0.369, crystals are also studied throughout 108–500 K temperature range. We have demonstrated that acentrosymmetric structure of these crystals does not transform to centrosymmetric β-polytype structure with mixing ratio and temperature and the crystals are still useful for nonlinear application. $GaSe_{1-x}S_x$, $x = 0.090–0.362$, crystals shown 15 to 30% higher damage threshold to that of pure GaSe crystals and up to 240% in SHG efficiency. Temperature dispersions of phase matching from $d\theta/dT = –4.9''/1$ °C to $22''/1$ °C and phase matching temperature bandwidth from 22 °C·cm to 219 °C·cm FWHM are determined, so as 2-fold improvement in hardness at $x = 0.1$ and 4-fold at $x = 0.4$ to that of pure GaSe.

1. Introduction

The *p*-type ε-GaSe is a highly birefringent ($B = 0.35$ at $\lambda = 10.6$ μm) and efficient nonlinear material. It can be phase matched (PM) for both type I and type II second harmonic generation (SHG), combination frequency and optical parametric generation [1] possessing generation of coherent light beams with extremely wide wavelength tuning from 0.954 [2] to 5664 μm [3], excluding narrow gap between 38.4 and 58.2 μm [3]. Unfortunately, the GaSe crystal is characterized by nearly zero hardness by Mohs scale, high cleavage and significant irreproducibility of nonlinear properties from sample to sample from 23 to 54 pm/V [1] and further to 70 pm/V [4].

On the other hand, the GaSe lattice well incorporates different doping elements, such as indium (In) [4, 5] and sulfur (S) [6–9] with noticeable modification of mechanical and nonlinear properties to that of pure GaSe. Single crystals of highly S-doped $GaSe_{1-x}S_x$ solids or the crystals, which are grown in accordance with chemical formula $GaSe:GaS \rightarrow GaSe_{1-x}S_x$ with mole mixing ratio (MR) $0.01 \le x \le 1$, are of special interest because three main reasons. First, they are the only crystals with end GaSe that form continuous series of solid solution crystals with x [10, 11] allowing to control its physical properties at the stage of growth process. Second, they are the only crystals that can meet the requirements for nonlinear optical devices pumped by high peak power all-solid-state near IR lasers due to shorter wavelength shift of transparency range with x [7]. And third, they have improved crystal structure and nonlinearity to pure ε-GaSe. In particular, $GaSe_{1-x}S_x$ possessing mechanical cut and polishing [6–9] and higher efficiency of SHG [8, 9]. There is extensive literature for the refractive indices dispersions in pure GaSe [1, 12–14], and a few papers reported for refractive indices dispersions in pure GaS for visible and near IR range ($\lambda \le 1$ μm) [15–17]. But so far, no one paper for dispersion or PM properties in the solid solution $GaSe_{1-x}S_x$ crystals versus x or temperature is published and no comparison is made for damage threshold and efficiency versus x. Even polytype structure change with mixing ratio was not studied through nonlinear measurement. Experimental results on frequency conversion in mixed crystal $GaSe_{1-x}S_x$, $x = 0.2$, 0.4 and, in contradiction to data on the crystal structure [18–21] even for $x = 0.8$, were reported only in one study [18].

[1] The work was supported by NSFC (Nos. 10334010, 10774059), the doctoral program foundation of institution of High Education of China and the National Basic Research Program (2006BC921103), joint Grant of RBRF (No. 07 02 92001 HHC_a) and NSCT (No. 96WFA0600007). One of the authors (G.L.) also gratefully acknowledges Russian Science Support Foundation and Presidium SB RAS.

In present study we report the optical and PM properties for SHG in pure *p*-type GaSe and modified $GaSe_{1-x}S_x$, $x = 0.04$, 0.023, 0.090, 0133, 0.175, 0.216, 0.256, 0.362, 0.369, and 0.412, crystals through 108–500 K temperature range. Polytype structure was also studied through nonlinear measurements.

2. Model estimations

Our previous model estimations on PM in $GaSe_{1-x}S_x$ crystals with use of available dispersion equations for pure GaSe and GaS are reported in [22]. It was found that birefringence *B* dispersions are highly spread for pure GaSe at wavelength $\lambda < 1.5$–2 μm. Over the maximal transparency spectral range earlier published dispersion equations are resulting in higher *B* in spite of the fact that during this period lower quality crystals were grown and these crystals are occasionally possessing fewer lower *B*. Possible reason for that is formulating of disperse equations for n_e from nonlinear measurements on frequency conversion of laser radiation, which were often at the wavelength range $\lambda < 1.5$–2 μm but not from direct measurements due difficulties in prism fabrication from these soft materials. Transparency spectrum, refractive index dispersions and resulted PM conditions significantly vary within this spectral range due to variations in crystal stoichiometry and optical quality.

Later published dispersion equations describe dispersion properties of the crystals with moderate $\alpha \sim 0.1$–0.05 cm^{-1} over maximal transparency range with lower variations in optical properties at short-wavelength cut-off. It can be proposed that better crystal quality results in almost identical *B* at maximal transparency range. Most available experimental data on CO_2 laser SHG are well related with data estimated on the basis of dispersion equations reported in [23]. SHG PM diagrams for mixed $GaSe_{1-x}S_x$ crystals estimated in this study are displayed in Fig. 1 in comparison with PM diagrams for moderate quality pure GaSe crystals [23].

Available data on GaS dispersion properties are limited by small wavelength range ≤ 1 μm [15–17] and so did not show here. In Fig. 1 it is seen that SHG PM diagrams estimated for centrosymmetric GaS and $GaSe_{1-x}S_x$ crystals with use the dispersion data of [23] are in unrealistic position to that of pure GaSe crystal. GaS birefringence is noticeably higher or at least similar to that of GaSe and it short-wavelength transparency end is at 0.48 μm for GaS in difference to 0.62 μm for GaSe [18–21]. That is why shorter-wavelength position of GaS and $GaSe_{1-x}S_x$ PM diagrams without shift to upper phase matching angles may be supposed sooner. But in Fig. 1 shift of the $GaSe_{1-x}S_x$ PM diagrams versus *x* is noticeable to longer-wavelength range, so as shift to higher PM angles and it irregularity at wavelength range $\lambda < 7.62$ μm. In principle, it can be due to $GaSe_{1-x}S_x$ crystal polytype structure change with *x*.

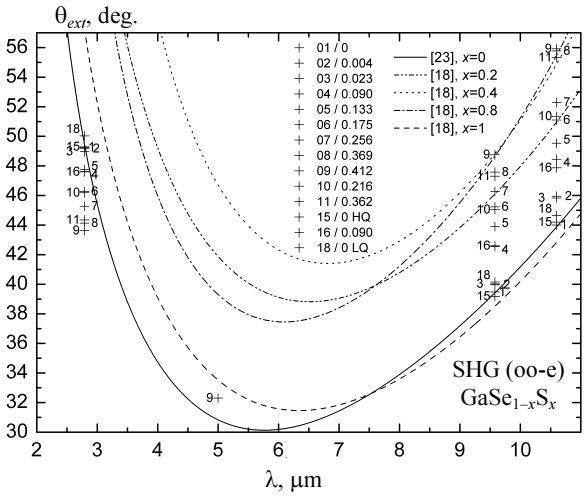

Fig. 1. SHG PM diagrams for pure GaSe after [13], $GaSe_{1-x}S_x$ after [7]. Points are this study experimental data for crystals studied (labeled in the figure inset by number reported in Table 1 of [23] mixing ratio)

Table 1. Parameters of GaSe and $GaSe_{1-x}S_x$ crystals and SHG PM angles

$GaSe_{1-x}S_x$			θ_{ext}, deg.		
No.	*x*	l_c, mm	2.79 μm	9.58 μm	10.6 μm
1	0	2.90	49.25	39.48	44.00
2	0.004	2.44	49.16	39.96	45.95
3	0.023	2.25	48.96	40.02	45.83
4	0.090	3.90	47.62	42.55	48.44
5	0.133	0.96	47.74	43.90	49.53
6	0.175	1.86	46.26	45.23	51.10
7	0.256	1.76	45.27	46.27	52.29
8	0.369	1.66	44.13	47.58	55.77
9	0.412	6.90	43.62	48.75	55.91
10	0.216	1.14	46.18	45.04	51.35
11	0.362	0.64	44.35	47.30	55.32
15	0	0.44	49.29	39.18	44.20
16	0.090	2.9	47.59	42.60	47.87
18	0	3.11	50.03	40.15	44.64

3. Experimental details

Pure GaSe and $GaSe_{1-x}S_x$ single crystals used in this study were grown by the Bridgeman–Stockbarger method [7]. Sliced off samples (Table 1) have been used without any additional treatment and polishing and some of them had visual defects such as broken layers and local layer pieces on the lone of high optical quality faces.

Electron probe microanalysis was used to determine *x* of these crystals. The $GaSe_{1-x}S_x$ crystals with different *x* form red to yellow color with respect to the increase of the sulfur composition. Transparency spectra were recorded through the $\Delta\lambda = 0.2$–0.9 μm and

$\Delta\lambda$ = 2.5–25 μm ranges with 0.05 nm and $\Delta\nu$ = 4 cm^{-1} spectral resolution, respectively. Point measurements with CO_2 laser exclude an influence of surface defects on the absorption coefficient estimations and show that for all crystals $\alpha \le 0.1$–0.2 cm^{-1} that could not be determined with higher accuracy due to small thickness of the crystals. The only pure GaSe crystal No. 18 has $\alpha \approx 0.25$ cm^{-1}. Traditional SHG optical setup was used and carefully expanded in [24].

4. Result and discussions

It was found that transparency spectra for $GaSe_{1-x}S_x$, x = 0–0.405, crystals are linearly shifting toward shorter wavelength with x, as it was supposed accounting shorter-wavelength transparency cut-off of GaS [19]. Specifically, short-wavelength transparency end shifts from 0.62 to 0.56 μm for the crystals studied but long-wavelength transparency end shifts from 18 to 14 μm. At once PM angles are gradually decreasing versus x for Er^{3+}:YSGG SHG and gradually increasing for CO_2 laser SHG (Table 1). Step changes in SHG efficiencies were also not observed. Linear shift of the wavelength transparency ends, gradual shift of Er^{3+}:YSGG and CO_2 laser SHG PM angles and SHG efficiency with x confirms that p-type $GaSe_{1-x}S_x$ studied is a continuous series of mixed crystals without change of polytype structure which is in agreement with data of [19, 21]. The spectral derivative of PM diagram at Er^{3+}:YSGG laser wavelength (Fig. 1) is a few times higher to spectral derivative at CO_2 laser wavelengths, but PM angle changes with x for Er^{3+}:YSGG SHG is about a half to changes for CO_2 laser SHG.

It can be explained by small (~ 0.07 μm) shift of short-wavelength transparency end in comparison with ~ 4.0 μm shift of long-wavelength transparency end of $GaSe_{1-x}S_x$ crystals towards shorter wavelength. PM angles for 3–5 μm OPO shown that only small shift to upper PM angles occurs that is in conflict with [18] but that is in good accord with GaSe and GaS birefringence meanings. Small increasing of PM angles possibly is caused by small changes of $GaSe_{1-x}S_x$ lattice parameters that is well known fact [19, 21]. No evident domain structure of the crystals was found. The error margin of ± 15–20″ of the measurements was due to local deformations of the crystal surfaces and long time instabilities of the facility parts.

In Fig. 2 it is seen that at positive temperatures PM angle for Er^{3+}:YSGG laser SHG are linearly increasing with temperature for all crystals. For GaSe No. 1 the slope $d\theta/dT$ = 22″/1 °C, it is of 19.4″/1 °C for $GaSe_{0.91}S_{0.09}$, 19″/1 °C for $GaSe_{0.825}S_{0.175}$ and 13″/1 °C for $GaSe_{0.631}S_{0.369}$ crystals, thus open lower temperature dependence of PM for mixed crystals versus x to that for pure GaSe. At the temperature range close to 108 K the slopes are of about a half to that at positive temperatures, thus shows birefringence decreasing as it was observed for $ZnGeP_2$ [19].

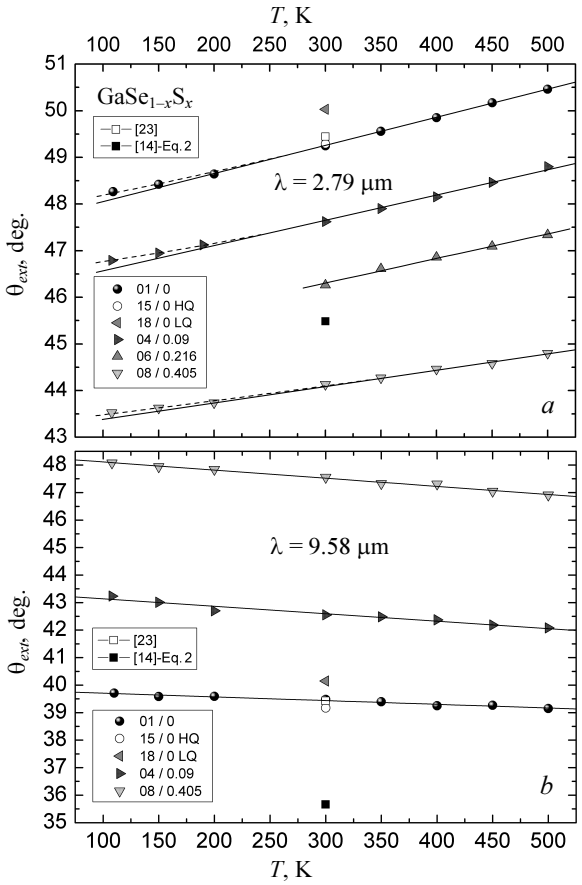

Fig. 2. External PM angles for SHG of Er^{3+}:YSGG (*a*) and 9.58 μm CO_2 laser emission line (*b*) versus temperature. Solid lines are approximations. Squared points are PM angles estimated with available data for refractive indices, LQ (HQ) is low (high) quality. Crystals studied/the crystals mixing ratios and references cited are identified in the figure insets

Measured PM temperature bandwidth in $GaSe_{0.91}S_{0.09}$ is of 22 °C · cm FWHM. In Fig. 2, *b* it is seen that PM angles for CO_2 laser SHG are linearly decreasing with temperature. For pure GaSe No. 1 the slope $d\theta/dT$ = = –4.9″/1 °C and it is something higher for mixed crystals: –9.7″/1 °C for $GaSe_{0.91}S_{0.09}$ and –10.6″/1 °C for $GaSe_{0.631}S_{0.369}$. PM temperature bandwidth for $GaSe_{0.91}S_{0.09}$ crystal at 9.58 μm is of 219 °C · cm FWHM that is close to the data of 172 °C · cm FWHM for pure GaSe crystal at 10.59 μm [13].

At room temperature PM angles are linearly changing with x both for Er^{3+}:YSGG and CO_2 laser SHG (Fig. 2) thus confirm that acentrosymmetric structure of the studied p-type crystals does not transform with x to centrosymmetric β-politype structure. Linear changing of PM with temperature indicates that the structure transformation do not appear at crystals temperature variation within 108–500 K. It is seen also from Fig. 1 that PM angle at the Er^{3+}:YSGG laser wavelength is decreasing with x and it is increasing at the CO_2 laser wavelength with the slope $|d\theta/dx|$ about 2-fold to that at Er^{3+}:YSGG laser wavelength.

But simultaneously, for SHG PM diagrams estimated slopes $d\theta/d\lambda$ at CO_2 laser and Er^{3+}:YSGG laser are rationed in inverse proportionality as 1:4. So, SHG PM diagrams for $GaSe_{1-x}S_x$ crystals are concurrently shifting with x toward shorter-wavelength range and toward higher PM angle range in full consent with shorter wavelength transparency cut-off of GaS and its lower birefringence in relation to GaSe crystal.

Direct comparison of damage thresholds and SHG efficiencies at Er^{3+}:YSGG and CO_2 laser wavelengths shown 15 to 30% higher damage threshold to that of pure GaSe crystals and up to 240% in SHG efficiency.

5. Conclusion

High optical quality, $\alpha \le 0.1–0.2$ cm^{-1}, mixed single crystals of p-type $GaSe_{1-x}S_x$, $x = 0.04$, 0.023, 0.090, 0133, 0.175, 0.216, 0.256, 0.362, 0.369, and 0.412, are grown and studied. Through transparency spectra, PM conditions and efficiency for Er^{3+}:YSGG and CO_2 laser SHG at room temperature it was determined that polytype structure of the p-type $GaSe_{1-x}S_x$ is not changing with x in spite of predominantly different polytype structure of end GaSe and GaS crystals at room temperature. These crystals are useful for application in nonlinear devices. SHG PM diagrams for $GaSe_{1-x}S_x$ crystals are simultaneously shifting with x to shorter-wavelength range in full consent with shorter wavelength transparency cut-off of GaS and possibly to upper position, as it goes from available data. It was shown that up to 1° difference in SHG PM angles can be caused by the difference in the GaSe astoichiometry.

We have reported the temperature dependent PM conditions for Er^{3+}:YSGG and CO_2 laser SHG in pure p-type ε-GaSe and mixed $GaSe_{1-x}S_x$, $x = 0.09$, 0.175, and 0.369, crystals throughout 108–500 K temperature range. From linear changing of phase matching angles with mixing ratio within $0 \le x \le 0.369$ and with temperature change within 108–500 K it can be concluded that acentrosymmetric structure of these crystals does not transforms to centrosymmetric β-polytype structure and the crystals are useful for nonlinear optical application. As low temperature dispersions of PM as from 22″/1 °C down to $d\theta/dT = –4.9''/1$ °C are determined at wide temperature PM temperature bandwidth of from 22 °C·cm to 219 °C · cm FWHM. Thus, in our knowledge, these crystals are of the most attractive for design of high power frequency converters at 2.79–10.6 μm pump due temperature insensitivity of phase matching conditions. Direct comparison of damage thresholds and SHG efficiencies at Er^{3+}:YSGG and CO_2 laser wavelengths shown 15 to 30% higher damage threshold to that of pure GaSe crystals and up to 240% in SHG efficiency.

References

[1] N.C. Fernelius, Prog. Crystal Growth Charact. **28**, 275 (1994).

[2] P. Kupecek and E. Batifol, Opt. Commun. **11**/3, 291 (1974).

[3] Y.J. Ding and W. Shi, Laser Phys. **16**/4, 562 (2006).

[4] D.R. Suhre, N.B. Singh, V. Balakrishna, N. Fernelius, and F. Hopkins, Opt. Lett. **22**/11, 775 (1997).

[5] N.B. Singh, D.R. Suhre, W. Rosch, R. Meyer, M. Marable, N.C. Fernelius, F. Hopkins, D. Zelmon, and R. Narayanan, J. Cryst. Growth. **198**, 588 (1999).

[6] S. Das, C. Ghosh, O.G. Voevodina, Yu.M. Andreev, and S.Yu. Sarkisov, Appl. Phys. B **82**, 43 (2006).

[7] Yu.M. Andreev, V.V. Atuchin, G.V. Lanskii, A.N. Morozov, L.D. Pokrovsky, S.Yu. Sarkisov, and O.V. Voevodina, Mat. Sci. Eng. B **128**, 205 (2006).

[8] S. Das, Ch. Ghosh, S. Gangopadhyay, U. Chatterjee, G.C. Bhar, V.G. Voevodin, and O.G. Voevodina, J. Opt. Soc. Am. B. **23**/2, 282 (2006).

[9] S. Das, C. Gosh, and S. Gangopadhyya, Infrared Phys. and Technol. **51**, 9 (2007).

[10] M. Schluter, J. Camassel, S. Kohn, Y. Shen, M. Cohen, and J. Voitchovsky, Phys. Rev. B. **13**, 3534 (1976).

[11] C.H. Ho, C.C. Wu, and Z.H. Cheng, J. Cryst. Growth. **279**, 321 (2005).

[12] N. Singh, D. Suhre, V. Balakrishna, M. Marable, R. Meyer, N. Fernelius, F. Hopkins, and D. Zelmon, Prog. Cryst. Growth Charact. Mat. **37**, 47 (1998).

[13] E. Takaoka and K. Kato, Jap. J. Appl. Phys. **38**, 2755 (1999).

[14] K.R. Allakhverdiev, T. Baykara, A. Kulibekov Gulubayov, A.A. Kaya, J. Goldstein, N. Fernelius, S. Hanna, and Z. Salaeva, J. Appl. Phys. **98**, 093515 (2005).

[15] T. McMath and J. Irwin, Phys. Stat. Sol. A **38**, 731 (1976).

[16] T.A. McMath, G. Jackle, and J.C. Irwin, Phys. Stat. Sol. A. **43**, K151 (1977).

[17] D. Errandonea, A. Segura, V. Munoz, and A. Chevy Phys. Rev. B **60**/23, 15866 (1999).

[18] K. Allakhverdiev, F. Ismailov, L. Kador, and M. Braun, Solid State Commun. **104**, 1 (1997).

[19] H. Serizawa, Yo. Sasaki, and Yu. Nishina, J. Phys. Soc. Jpn. **48**, 490 (1980).

[20] K.R. Allakhverdiev, R.I. Guliev, E.Yu. Salaev, and V. Smirnov, Sov. J. Quant. Electron. **12**, 947 (1982).

[21] C. Pérez León, L. Kador, K.R. Allakhverdiev, T. Baykara, and A. Kaya, J. Appl. Phys. **98**, 103103 (2005).

[22] H. Zhang, Z. Kang, Y. Jiang, J. Gao, F. Wu, Z. Feng, Yu. Andreev, G. Lanskii et. al., "SHG phase matching in GaSe and mixed $GaSe_{1-x}S_x$, $x \le 0.412$, crystals at room temperature", Opt. Express [in press].

[23] K.L. Vodopyanov, and L.A. Kulevskii, Opt. Commun. **118**, 375 (1995).

[24] Z.-S. Feng, Z.-H. Kang, F.-G. Wu, J.-Y. Gao, Y. Jiang, H.-Z. Zhang, Yu. Andreev, G. Lanskii, V. Atuchin, and T. Gavrilova, "SHG in doped GaSe:In crystals", Opt. Express [in press].